

Evaluation of the Kuz-Ram Model and Its Extensions for Predicting Fragmentation Size Distribution from Blasting: Case Study of the Diack Basalt Quarry (Senegal)

Lamine BAR*, Déthié SARR, Hamed FALL, Makhtar SOW

Geotechnical Department, L2M, UFR of Engineering Sciences, Iba Der Thiam University, Thies-Senegal

*Corresponding author: lamine.bar@univ-thies.sn

Received March 01, 2026; Revised April 01, 2026; Accepted April 08, 2026

Abstract This study evaluates the predictive performance of the Kuz-Ram model and its extensions (Shifted Kuz-Ram and Extended Kuz-Ram) for blast-induced fragmentation in a hard rock geological context: the Diack basalt quarry in Senegal. Particle size distributions were obtained through WipFrag® image analysis and compared to model predictions. The results show that the original Kuz-Ram model (1987) reproduces the general trend with an R^2 of 0.91 but underestimates the mid-size range. The introduction of the shifting factor (Shifted Kuz-Ram) significantly improves the fit ($R^2 = 0.96$). The Extended Kuz-Ram model by Cunningham (2005), after calibration of the $C(A)$ and $C(n)$ coefficients, offers the best performance with an R^2 of 0.995 and an RMSE of 2.76%, demonstrating the importance of local adaptation of empirical parameters. This study contributes to optimizing blast design in basaltic environments and highlights the necessity of calibrating models with field data.

Keywords: Blast fragmentation, Kuz-Ram model, Extended Kuz-Ram, Diack quarry, WipFrag® image analysis

Cite This Article: Lamine BAR, Déthié SARR, Hamed FALL, and Makhtar SOW, "Evaluation of the Kuz-Ram Model and Its Extensions for Predicting Fragmentation Size Distribution from Blasting: Case Study of the Diack Basalt Quarry (Senegal)." *American Journal of Mining and Metallurgy*, vol. 9, no. 1 (2026): 7-14. doi: 10.12691/ajmm-9-1-2.

1. Introduction

Blasting is a key operation in mining and quarrying, as it directly conditions the productivity of downstream operations (loading, hauling, crushing) and strongly influences energy consumption and operating costs [1,2]. The resulting particle size distribution (fragmentation) from a blast is therefore a critical parameter for optimizing the mine-to-mill chain; improving fragmentation reduces grinding energy and increases crusher productivity [2]. Accurate prediction of post-blast particle size distribution is essential for optimizing blast parameters (burden, spacing, explosive charge) and adapting downstream processes, particularly in varied geological contexts such as hard igneous rocks (basalt) [3]. In Senegal, aggregate quarrying supports a booming construction sector, but the lack of predictive approaches adapted to local lithologies often hinders yield optimization.

Initial theoretical approaches date back to the work of Kuznetsov [4] on mean fragment size and Rosin & Rammler [5] on the particle size distribution function. Cunningham synthesized these approaches into the Kuz-Ram model [6,7], which combines Kuznetsov's equation for mean size and the Rosin-Rammler function for

distribution. This model is widely used for blast design and fragmentation assessment. Subsequently, Spathis [8] proposed a correction concerning the confusion between mean size and median size, which led Ouchterlony [9] to introduce a shifting factor into the model, giving rise to the Shifted Kuz-Ram. Cunningham [10] also proposed an extended version of the model (Extended Kuz-Ram) incorporating the effect of timing and delay scatter on fragmentation.

Despite these developments, discrepancies persist between predictions and field measurements due to local geological variability, blast parameters, and explosive characteristics. It is therefore necessary to evaluate these models on specific contexts, such as the massive basalt of Diack, to identify the most robust method.

In this context, the present study systematically compares the performance of three models from the Kuz-Ram family: (i) the original model by Cunningham [7], (ii) the Shifted Kuz-Ram model as formalized by Ouchterlony [9], and (iii) the Extended Kuz-Ram model by Cunningham [10]. The evaluation is carried out at the Diack quarry (basalt) in Senegal. Reference particle size curves were obtained through WipFrag® image analysis after blasting.

The objective is twofold: (i) to examine each model's ability to reproduce measured particle size distributions,

and (ii) to identify the model best suited to the basaltic context. This work helps fill the lack of comparative studies applied to Senegalese rocks and provides a scientific basis for future optimization of blast parameters.

2. Methodology

2.1. Study Site and Geological Characterization

The Diack quarry is located in the Ngoudiane municipality, approximately 37 km southeast of Thiès (Senegal). Figure 1 shows the quarry location. It exploits massive, dense, and resistant volcanic basalt from the Tertiary volcanism of the region. This basalt presents several facies ranging from fine to coarse, influencing its hardness and mechanical properties [11]. Due to its compactness and low porosity, it serves as a reference in Senegal for the production of high-performance aggregates [12].

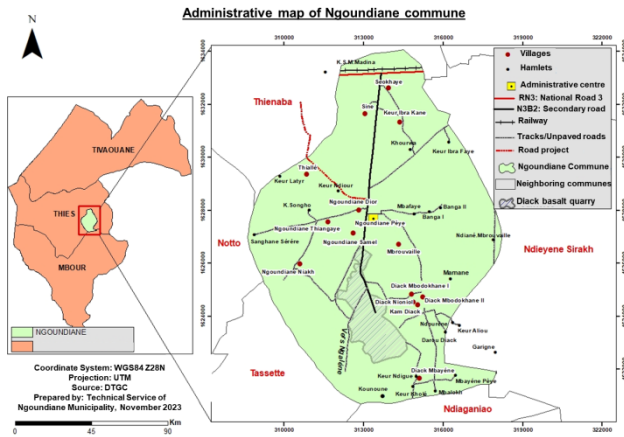


Figure 1. Location of the Diack quarry (Technical Service of the Ngoudiane Municipality, 2023)

2.2. Acquisition and Processing of Particle Size Data

Actual particle size distributions were obtained through image analysis after blasting. For the blast, a total of 15 photographs of the blasted face were taken with a digital camera, placing a foldable wooden measuring rule folded to form a 22 cm square as a scale object. The sampling strategy followed the recommendations of the WipWare : each image was framed to contain at least 400 fragments, and systematic coverage of the muckpile was performed to ensure statistical representativeness. This protocol reduces biases related to camera angle and image representativeness [13,14]. Figure 2 illustrates the blasted muckpile at the Diack quarry.

The calibrated images were then processed with WipFrag® software to automatically detect fragment outlines and generate cumulative particle size curves (cumulative % passing vs. size in mm). Several images from this blast were averaged to obtain a representative distribution, according to practices described by Nanda & Naik [15]. Figure 3 shows the particle size curve obtained for the Diack basalt.

This measured distribution serves as the baseline reference for comparison with predictions generated by the empirical fragmentation models.

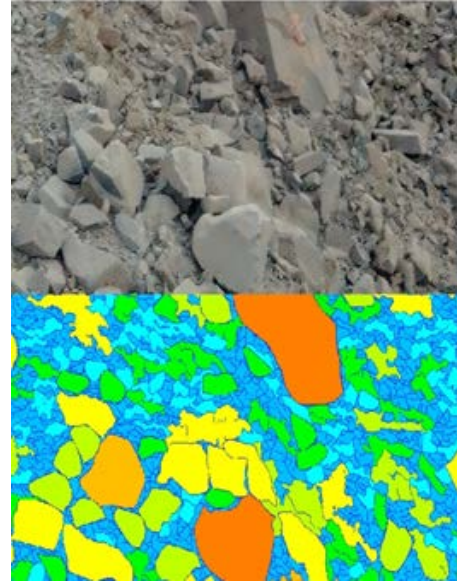


Figure 2. Muckpile after blasting at the Diack basalt quarry, processed with WipFrag®

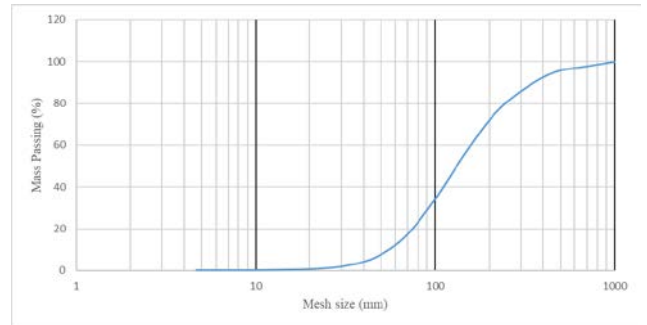


Figure 3. Granulometric Curves of the Diack Basalt Quarry from WipFrag® Analysis

2.3. Fragmentation Models and Theoretical Formulations

2.3.1. Kuz-Ram Model [7]

The Kuz-Ram model combines the Kuznetsov [4] equation for mean fragment size x_m and the Rosin & Rammler [5] distribution function.

The mean size is calculated by the following Kuznetsov–Cunningham equation:

$$x_m = A \times q^{-0.8} \times Q^{1/6} \times \left(\frac{115}{RWS} \right)^{19/30} \quad (1)$$

where x_m is the mean size (cm), q is the powder factor (kg/m^3), Q is the explosive charge per hole (kg), RWS is the relative weight strength compared to ANFO, and A is the rock factor, reflecting the mechanical and structural characteristics of the rock mass. It can be estimated either by the formula proposed by Cunningham [7],

$$A = 0.06(RMD + RDI + HF) \quad (2)$$

or from the blastability index (Lilly [16]) with

$$A = 0.12 \times BI .$$

The particle size distribution is described by the Rosin-Rammler function:

$$R_x = 1 - \exp \left[-0.693 \left(\frac{x}{x_m} \right)^n \right] \quad (3)$$

where R_x represents the cumulative fraction passing a sieve of mesh size x , and n is the uniformity index, which controls the fragment uniformity. The latter is calculated by:

$$n = (2.2 - 0.014B / \phi_h) \times \left(1 - \frac{SD}{B} \right) \times \sqrt{\left[(1 + S / B) / 2 \right]} \times \left[\frac{|L_b - L_c|}{L_{tot}} + 0.1 \right]^{0.1} \times (L_{tot} / H) \quad (4)$$

where B is the burden (m), S is the spacing between holes (m), ϕ_h is the hole diameter (m), L_b is the bottom charge length (m), L_c is the column charge length (m), L_{tot} is the total charge length, possibly above ground level (m), H is the bench height (m). According to Olofsson [17], the drilling deviation SD (m) can be estimated using the relation: $SD = \phi_h + 0.03L$, with L being the hole depth (m).

2.3.2. Shifted Kuz-Ram Model [9]

To correct certain biases observed in the original Kuz-Ram model, Spathis [8] introduced a variant based on the introduction of a shifting factor $g(n)$. This approach was subsequently formalized and named the Shifted Kuz-Ram model by Ouchterlony [9].

In this version, the Kuznetsov–Cunningham function is modified by introducing a shifting factor $g(n)$, which essentially shifts the particle size distribution towards smaller x_{50} values or leads to predicting more fines [8].

The proposed equation linking the median size x_{50} to the mean size x_m is:

$$x_{50} = g(n) \times x_m \quad (5)$$

with

$$g(n) = \frac{(\ln 2)^{1/n}}{\Gamma(1 + 1/n)} \quad (6)$$

where Γ is the mathematical Gamma function.

It should be noted that the introduction of the shifting factor $g(n)$ by Ouchterlony [9] aimed primarily to correct the confusion between mean size x_m and median size x_{50} pointed out by Spathis [8]. Nevertheless, as highlighted by Ouchterlony & Sanchidrián [18], the revised equations of the Kuz-Ram model [7] had already been calibrated directly on x_{50} data.

Nevertheless, its use may remain relevant as it allows shifting the Kuz-Ram model towards a prediction closer to the measured particle size distribution. This precision underscores that subsequent developments of the Kuz-Ram model essentially rely on predicting the median size x_{50} , which reinforces its statistical coherence and operational use.

2.3.3. Extended Kuz-Ram Model [10]

In his article "The Kuz-Ram fragmentation model -- 20 years", Cunningham [10] summarizes and adjusts the classic Kuz-Ram formulations, explicitly introducing the effect of timing and delay scatter on fragmentation (via factors A_t and the scatter ratio) [10,19]. These additions aim to make the model more accurate in modern blasting contexts (electronic detonators, delay control) [10,19].

Equation (1) for the mean fragment size is modified according to:

$$x_m = AA_t q^{-0.8} Q^{1/6} \left(\frac{115}{RWS} \right)^{19/30} C(A) \quad (7)$$

with

• A_t : time dispersion factor which depends on the ratio T/T_{max} . For T/T_{max} between 0 and 1:

$$A_t = 0.66 \left(\frac{T}{T_{max}} \right)^3 - 0.13 \left(\frac{T}{T_{max}} \right)^2 - 1.58 \left(\frac{T}{T_{max}} \right) + 2.1 \quad (8)$$

and for $T/T_{max} > 1$:

$$A_t = 0.9 + 0.1 \left(\frac{T}{T_{max}} - 1 \right) \quad (9)$$

Here, T is the actual delay between consecutive holes in the same row (ms), and T_{max} is the optimal value for this delay. Factor A_t plays an empirical modulation role on fragmentation according to blast synchronization. The idea is that optimal detonation synchronization improves fragmentation, while delays that are too short or too long degrade it [10].

The optimal delay is approximately given by:

$$T_{max} = \frac{15.6}{C_p} B \quad (10)$$

where C_p is the longitudinal wave velocity (km/s), B is the burden (m), and the coefficient 15.6 comes from empirical calibration combining propagation time values and experimental scale.

• $C(A)$: correction factor for the rock factor, ranging between 0.5 and 2.

The uniformity equation (4) is modified to integrate precision effects (delay scatter):

$$n = n_s \times \left(\frac{A}{6} \right)^{0.3} \times \sqrt{\left(2 - \frac{30B}{\phi_h} \right)} \times \sqrt{\frac{1 + S/B}{2}} \times \left(1 - \frac{SD}{B} \right) \times \left(\frac{L_{tot}}{H} \right)^{0.3} \times C(n) \quad (11)$$

where $C(n)$ is a correction factor used to adjust the uniformity index when it does not match algorithm predictions, and n_s is the uniformity factor determined by the scatter ratio in equation [10].

Indeed, Cunningham also introduces the effect of timing scatter and proposes the concept of scatter ratio R_s :

$$R_s = \frac{T_r}{T_x} = 6 \frac{\sigma_t}{T_x} \quad (12)$$

which moderates the uniformity index when scatter is significant. In this way, the model considers not only the blast parameters but also the execution quality of the initiation system.

Note that $C(A)$ and $C(n)$ are multiplicative factors used to adapt/calibrate the equations to site-specific conditions [19].

Finally, Cunningham [10] maintains the use of the Rosin-Rammler particle size distribution, as defined by equation (3), despite certain criticisms [9,18].

2.3.4. Model Calibration

Table 1. Blast parameters and rock mass properties at Diack

Parameter	Value	Unit
Burden (B)	4	m
Spacing (S)	4	m
Bench height (H)	12.9	m
Hole diameter (ϕ_h)	102	mm
Bottom charge length (L_b) (above ground level, i.e., without subdrilling)	1.04	m
Column charge length (L_c)	10.36	m
Total charge length (L_{tot}) (with subdrilling)	11.9	m
Hole depth (L)	13.4	m
Rock factor (A)	5.34	-
Rock Mass Description (RMD)	50	-
Hardness factor (HF)	24	-
Rock Density Influence (RDI)	15	-
Powder factor (q)	0.4017	kg/m ³
Charge per hole (Q)	82.92	kg
RWS (ANFO)	100	-
Wave velocity (C_p)	5038.315	m/s
Inter-hole delay (T)	25	ms
Delay standard deviation (σ_t)	5	ms

For the Extended model, coefficients $C(A)$ and $C(n)$ were numerically optimized by minimizing the root mean square error between predictions and WipFrag® measurements. For the other models, no additional

adjustments were applied beyond the field-measured input parameters (Table 1).

3. Analysis of Results

The particle size distributions measured at the Diack quarry (Figure 3) were compared to the predictions of the three models. The performance indicators used are the coefficient of determination (R^2), root mean square error (RMSE), mean absolute error (MAE), and standard error of estimate (SEE).

3.1. Original Kuz-Ram Model

The model by Cunningham [7] gives a mean size $x_m = 230.17$ mm and a uniformity index $n = 1.26$. The overall fit is satisfactory ($R^2 = 0.91$), but an underestimation of particles in the 100–464 mm range is observed, with a mean error of 6.38% and an RMSE of 12.27% (Figure 4).

3.2. Shifted Kuz-Ram Model

The application of the shifting factor reduces the median size to $x_{50} = 185.40$ mm, for the same index $n = 1.26$. The fit quality improves significantly with $R^2 = 0.96$, RMSE = 7.89%, and MAE = 5.47% (Figure 5). The underestimation of the mid-size particles is corrected, but a slight overestimation of very fine fractions (< 68 mm) appears.

3.3. Extended Kuz-Ram Model

Without calibration of coefficients $C(A)$ and $C(n)$ (default values = 1), the Extended model gives a mean size of 230 mm and a uniformity index $n = 0.59$ (below the usual limit of 0.7), with a poor fit ($R^2 = 0.794$, RMSE = 18.4%). After numerical optimization, the retained values are $C(A) = 0.62$ and $C(n) = 2.83$, leading to $x_m = 142.4$ mm and $n = 1.67$. The fit becomes excellent: $R^2 = 0.995$, RMSE = 2.76%, MAE = 1.98% (Figure 6). The predicted curve coincides remarkably with the measurements over the entire particle size range.

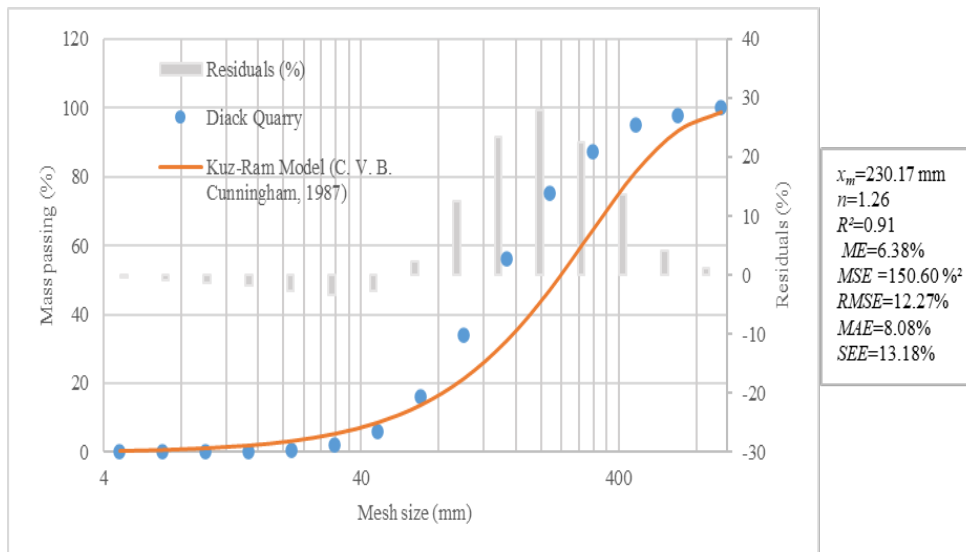


Figure 4. Grain Size Distribution and Prediction Performance for Diack Quarry vs. Kuz-Ram Model in lin-log Space

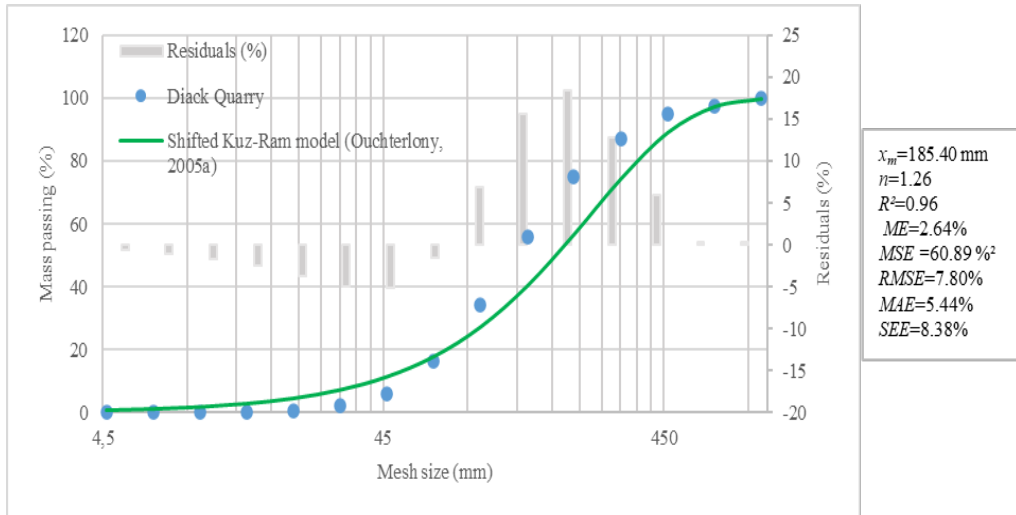


Figure 5. Grain Size Distribution and Prediction Performance for Diack Quarry vs. Shifted Kuz-Ram Model

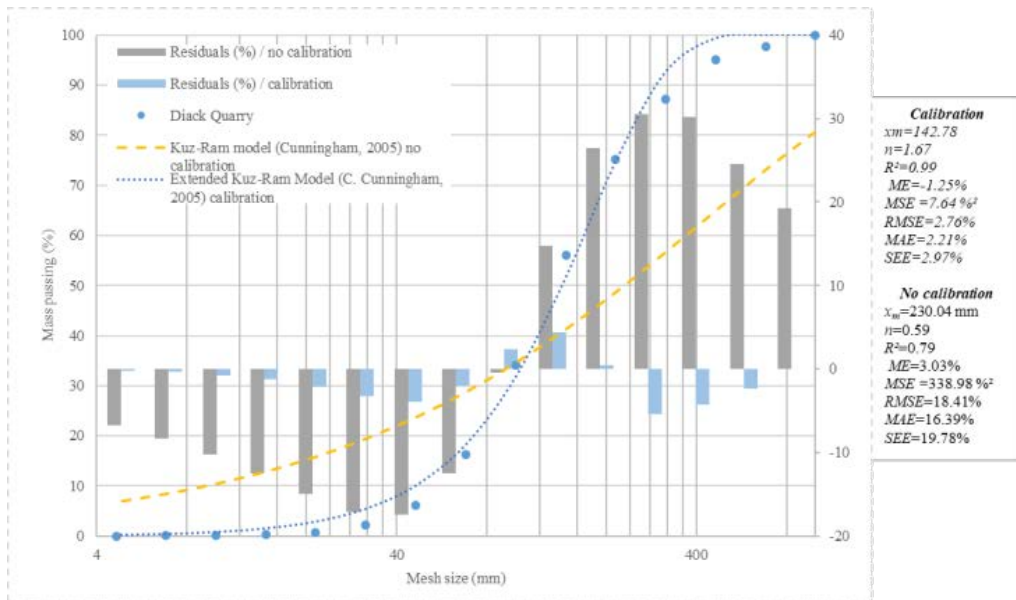


Figure 6. Grain size distribution and prediction performance for Diack Quarry compared to the Extended Kuz-Ram Model (C. Cunningham, 2005) in lin-log space. The curves show both the calibrated case ($C(A) = 0.62$; $C(n) = 2.83$) and the uncalibrated case ($C(A) = 1$; $C(n) = 1$), illustrating the impact of calibration on prediction accuracy

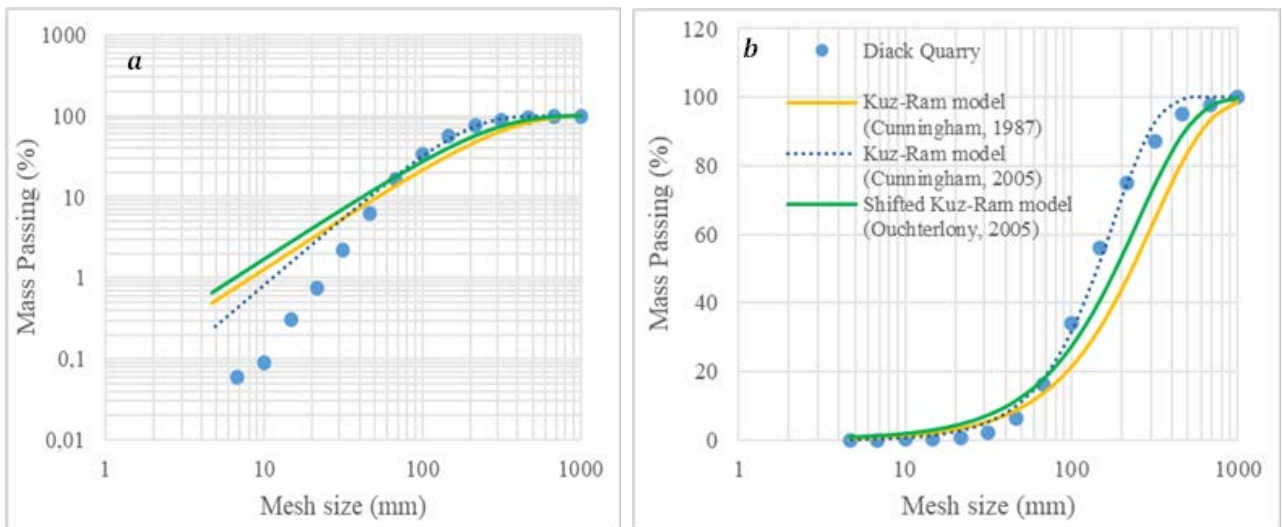


Figure 7. Grain Size Distribution Curves from Diack Quarry Compared with Prediction Methods: (a) log-log space, (b) lin-log space

3.4. Model Comparison

Figure 7 compares the particle size curves predicted by the three Cunningham models with the experimental measurements. The original model underestimates the intermediate fractions, the shifted model improves the fit, and the calibrated Extended model reproduces the measured distribution almost perfectly.

Table 2 summarizes the performance indicators for the three models.

Table 2. Performance indicators of the models for the Diack quarry

Modèle	x_{50} (mm)	n	R ²	RMSE (%)	MAE (%)	SEE (%)
Original Kuz-Ram	230.17	1.26	0.910	12.27	6.38	11.52
Shifted Kuz-Ram	185.40	1.26	0.960	7.89	5.47	7.41
Extended Kuz-Ram (uncalibrated)	230.0	0.59	0.794	18.4	12.1	17.3
Extended Kuz-Ram (calibrated)	142.4	1.67	0.995	2.76	1.98	2.59

3.5. Advanced Comparative Analysis of Cunningham Models

To refine the evaluation of the three Cunningham models applied to the Diack quarry, we adapted the scatter and Radar plots presented in Figure 8 and Figure 9.

Figure 8 presents a scatter plot of cumulative passing predicted by each model against measured passing. Points aligned on the first bisector indicate a perfect prediction. The results reveal contrasting trends at the study site. The models tend to overestimate the proportion of fine fragments, while intermediate size classes are often underestimated. It is observed that the calibrated *Extended Kuz-Ram* model comes closest to this ideal line, confirming its superiority. The *Shifted Kuz-Ram* shows moderate dispersion, while the *Original Kuz-Ram* shows more pronounced deviations for intermediate fractions.

Finally, Figure 9 normalizes several error metrics (R², R²_{adjus}, MSE, RMSE, MAE, SEE and ME) for each of the three models. This normalization highlights the relative performance gap. The calibrated Extended model shows the lowest errors across all criteria, underscoring its robustness for this lithological context.

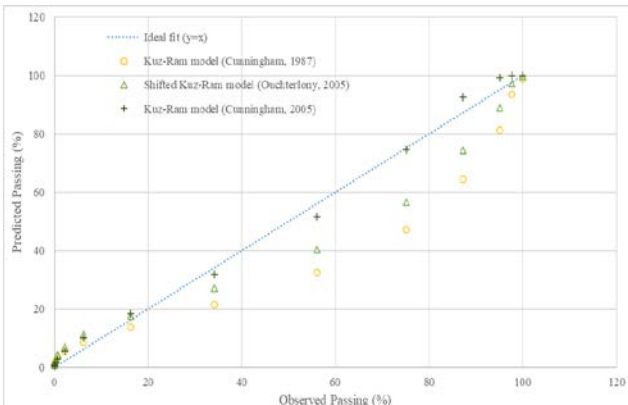


Figure 8. Diack quarry – Prediction Methods: Scatter Plot of Predicted vs. Observed Passing



Figure 9. Global Performance Comparison of Models

4. Discussion

The obtained results show that the performance of empirical fragmentation models varies significantly according to the degree of sophistication and applied calibration. In the context of the massive Diack basalt, the original Kuz-Ram model [7] provides an acceptable first approximation but with a marked underestimation in the intermediate size range (Figure 4). This bias is consistent with literature observations, which attribute this limitation to the confusion between mean size and median size, as well as the absence of consideration for the upper block size limit [18].

The introduction of the shifting factor $g(n)$ (Shifted Kuz-Ram) effectively corrects this error by bringing the median size to a more realistic value (185 mm instead of 230 mm). The improvement in fit (R² increases from 0.91 to 0.96) confirms the relevance of this correction for the Diack basalt. However, a slight overestimation of the finest fractions (< 68 mm) remains (Figure 5), which could be related to the shape of the Rosin-Rammler function, less adapted to the distribution tail [9].

The Extended Kuz-Ram model [10] proves to be the most effective, provided local calibration of coefficients C(A) and C(n) is performed. Without calibration, its results are even inferior to the original model (Figure 6), highlighting the danger of using default parameters. Calibration allowed optimizing these coefficients (0.62 and 2.83 respectively), leading to an almost perfect prediction (R² = 0.995). This improvement is explained by the consideration of the effect of timing and delay scatter, which are key factors in fragmentation control [10]. The C(A) value lower than 1 indicates that the effective rock factor is lower than the initial estimate, likely due to the natural fracturing of the rock mass.

The obtained value C(n)=2.83 is substantially higher than the default value of 1 [10] and reflects a greater uniformity than that predicted by the geometric parameters alone, which may be due to good blast synchronization. However, such a deviation from the default value warrants discussion. As noted by Ouchterlony and Sanchidrián [18], the validation of empirical fragmentation models requires multiple blasts, because the variability in blasting conditions can distort localized calibrations. The fact that this calibration was performed using data from a single blast may therefore contribute to the high value obtained. Future work

incorporating multiple blasts with varied blast designs will be necessary to determine whether this value reflects a genuine site-specific characteristic or a case of localized overfitting.

From a practical perspective, the choice between the three models depends on the trade-off between accuracy and implementation effort. The original Kuz-Ram model requires only basic blast parameters and is readily applicable for first estimates. The Shifted Kuz-Ram model adds a simple correction factor but remains easy to implement. In contrast, the Extended Kuz-Ram model, while offering the highest accuracy after calibration, requires detailed timing data and a calibration procedure, which may be justified for large-scale operations where fragmentation optimization yields significant downstream benefits.

These results align with other studies that have emphasized the importance of calibrating empirical models [19,20]. They also show that the Diack basalt, although massive, presents a certain heterogeneity requiring fine-tuning of parameters.

From a practical standpoint for blasting operations in this type of rock, the use of the calibrated Extended model is recommended. The calibration procedure can be performed from a few test blasts analyzed by WipFrag, as was done here. The shifted model, being simpler, constitutes an acceptable alternative when timing data are unavailable or calibration is not possible.

However, this study has certain limitations. It only covered a single site and a limited number of blasts. Additional investigations in other areas of the quarry and with different blast patterns would allow validating the robustness of the calibrated coefficients. Furthermore, WipFrag image analysis, although widely used, involves uncertainties related to segmentation and image representativeness [13,14]. Complementary measurements by sieving, although difficult on a large scale, could strengthen the reliability of the reference data.

Finally, the lack of consideration for the extreme fines distribution in Rosin-Rammler models could be mitigated by using more flexible functions like Swabrec [9], but this is beyond the scope of this study focused on Cunningham models.

5. Conclusion

This study evaluated three models from the Kuz-Ram family for predicting blast fragmentation at the Diack basalt quarry in Senegal. The results show that:

- The original Cunningham model [7] gives a correct global estimate but underestimates the mid-size range (Figure 4).
- The Shifted Kuz-Ram model [9] significantly improves accuracy by correcting the confusion between mean and median size (Figure 5).
- The Extended Kuz-Ram model [10], after calibration of coefficients $C(A)$ and $C(n)$, offers the best performance with an R^2 of 0.995 and an RMSE of 2.76% (Figure 6).

These results confirm the necessity of adapting empirical models to local conditions through calibration with field data. For the Diack basalt, the calibrated

Extended model constitutes the most reliable tool for optimizing blast parameters and improving operational profitability.

Future perspectives include extending this approach to other lithologies and integrating machine learning techniques to refine predictions. Coupling with numerical models (DEM, FEM) could also allow a better understanding of fragmentation mechanisms and overcome the limitations of purely empirical approaches.

References

- [1] Kinyua, E. M., Jianhua, Z., Kasomo, R. M., Mauti, D., & Mwangangi, J. (2022). A review of the influence of blast fragmentation on downstream processing of metal ores. *Minerals Engineering*, *186*.
- [2] Zhang, Z. X., Sanchidrián, J. A., Ouchterlony, F., & Luukkanen, S. (2023). Reduction of Fragment Size from Mining to Mineral Processing: A Review. *Rock Mechanics and Rock Engineering*, *56*(1), 747–778.
- [3] Mutinda, E. K., Alunda, B. O., Ondicho, I. O., & Agyekum, E. (2025). Prediction and measurement of blast induced rock fragmentation – A case study of Kajiado County quarries, Kenya. *Journal of the Southern African Institute of Mining and Metallurgy*, *125*(2), 113–120.
- [4] Kuznetsov, V. M. (1973). The mean diameter of the fragments formed by blasting rock. *Soviet Mining Science*, *9*(2), 144–148.
- [5] Rosin, P., & Rammler, E. (1933). The Laws Governing the Fineness of powdered coal. *Journal of the Institute of Fuel*, *7*, 29–36. <https://www.scrip.org/reference/ReferencesPapers?ReferenceID=2167099>.
- [6] Cunningham, C. V. B. (1983). The Kuz-Ram Model for Prediction of Fragmentation from Blasting. In R. Holmberg & A. Rustan (Eds.), *First International Symposium on Rock Fragmentation by Blasting* (pp. 439–453). Luleå University of Technology. <https://www.scrip.org/reference/referencespapers?referenceid=2271764>.
- [7] Cunningham, C. V. B. (1987). Fragmentation Estimations and the Kuz-Ram Model—Four Years on. In W. L. Fourney & R. D. Dick (Eds.), *Second International Symposium on Rock Fragmentation by Blasting* (pp. 475–487). <https://www.scrip.org/reference/referencespapers?referenceid=2271765>.
- [8] Spathis, A. T. (2004). A correction relating to the analysis of the original Kuz-Ram model. *Fragblast*, *8*(4), 201–205.
- [9] Ouchterlony, F. (2005). The Swabrec© function: Linking fragmentation by blasting and crushing. *Institution of Mining and Metallurgy. Transactions. Section A: Mining Technology*, *114*(1).
- [10] Cunningham, C.V.B. (2005) The Kuz-Ram Fragmentation Model—20 Years on. Brighton Conference Proceedings, European Federation of Explosives Engineers, Brighton, 13-16 September 2005, 201-210.
- [11] Dia, A. (1982). Contribution à l'étude des caractéristiques pétrographiques, pétrochimiques et géotechniques des granulats basaltiques : de la presqu'île du Cap-Vert et du Plateau de Thiès.
- [12] Bar, L., Sarr, D., A. Sall, O., & Gueye, E. H. M. (2025). Blasting Analysis on the Basalt of Diack (Senegal) Using the Langefors-Kihlstrom Theory. *International Journal of Research and Review*, *12*(4), 143–152.
- [13] Amin, I., & Salman, S. (2022). Fragmentation Analysis of Blasted Rock using WipFrag Image Analysis Software. *Journal of Mines, Metals and Fuels*, 263–267.
- [14] Maerz, N. H., Palangio, T. C., & Franklin, J. A. (1996). WipFrag image based granulometry system. *Measurement of Blast Fragmentation*, 91–99.
- [15] Nanda, S., & Naik, H. K. (2023). A Review of the Blast Fragmentation Analysis Techniques used in Surface Mines. *Journal of Mines, Metals and Fuels*, 2445–2454.
- [16] Lilly, P. A. (1986). EMPIRICAL METHOD OF ASSESSING ROCK MASS BLASTABILITY. *Symposia Series - Australasian Institute of Mining and Metallurgy*, 89–92.
- [17] Olofsson, S. O. (1991). Applied explosives technology for construction and mining. 304.

- [18] Ouchterlony, F., & Sanchidrián, J. A. (2019). A review of development of better prediction equations for blast fragmentation. *Journal of Rock Mechanics and Geotechnical Engineering*, *11*(5), 1094–1109.
- [19] Saldana, M., Gallegos, S., Arias, D., Salazar, I., Castillo, J., Salinas-Rodríguez, E., Navarra, A., Toro, N., & Cisternas, L. A. (2024). Applications of Kuz--Ram Models in Mine-to-Mill Integration and Optimization---A Review. *Minerals*, *14*(11).
- [20] Marinin, M. A., Afanasyev, P. I., Sushkova, V. I., Ustimenko, K. D., & Akhmetov, A. R. (2023). The experience of using the Kuz-Ram model in describing of grain size distribution of blasted rock mass. *Mining Informational and Analytical Bulletin*, (9-1), 96–109.



© The Author(s) 2026. This article is an open access article distributed under the terms and conditions of the Creative Commons Attribution (CC BY) license (<http://creativecommons.org/licenses/by/4.0/>).